INTEGRAL: A NEW GAMMA-RAY ASTRONOMY MISSION

B. J. Teegarden
Laboratory for High-Energy Astrophysics
NASA/Goddard Space Flight Center

ABSTRACT

INTEGRAL (International Gamma-Ray Astrophysics Laboratory) is a major new space observatory of the European Space Agency that was launched on Oct. 17, 2002. After successfully completing a 2-month commissioning period INTEGRAL began its scientific operations and continues to perform essentially flawlessly. The payload consists of two major instruments, a high-resolution cooled-germanium spectrometer (SPI) and a coded-aperture imager employing a large array of CdTe detectors (IBIS). Early science highlights include the detection of 12 new transient sources, possible identification of a new class of highly absorbed hard X-ray sources and the production of prompt and accurate locations of gamma-ray bursts.

1 THE INTEGRAL MISSION

INTEGRAL (International Gamma-Ray Astrophysics Laboratory) is a new observatory-class mission of the European Space Agency (ESA) designed to carry out astronomical gamma-ray observations in the 15-8000 keV interval. Launched in Oct. 2002, the spacecraft began normal science operations at the beginning of 2003 and has been performing smoothly since then. The two main instruments on board are a spectrometer (SPI) and an imager (IBIS). In addition there are two supporting monitor instruments an X-ray and an optical monitor (JEM-X and OMC). The use of new technology detectors (germanium in the case of the spectrometer and CdTe in the case of the imager) has resulted in significant improvements in energy and angular resolution over previously flown space experiments (c.f. Compton Gamma-Ray Observatory). INTEGRAL forms a complementary set with NASA's Swift and GLAST missions. When all three are operational (expected in 2-3 yr) there will be unprecedented coverage of the gamma-ray region of the celestial electromagnetic spectrum.

1.1 Spacecraft

The INTEGRAL spacecraft is shown in Fig. 1. The four instruments are all co-aligned and pointed at individual targets with an accuracy of a fraction of a fraction of an arcmin.

The fixed solar panels must be oriented within $\pm$ 40° of the sun which restricts the allowed pointing directions. Any given portion of the sky is typically visible for two 2-3 month periods each year. The only on-board consumable is the fuel required for unloading and biasing the reaction wheels and there is currently at least a 15-year supply. The spacecraft was launched on a Russian Proton vehicle into a high inclination orbit with an apogee of $\sim$110,000 km, an initial perigee of $\sim$10,000 km and a 3 day period. In this orbit the spacecraft never enters the trapped proton belts and is thus free from activation effects that have plagued prior spacecraft in low earth orbit. The overall instrument background, although somewhat higher than that in low earth orbit, is much more stable. The spacecraft pointing direction is nearly always moving in a dither pattern (typically a 5×5 grid with a separation between adjacent points of 2°) to effectively chop the beam and allow more accurate background determination as well as improve the quality of the imaging.

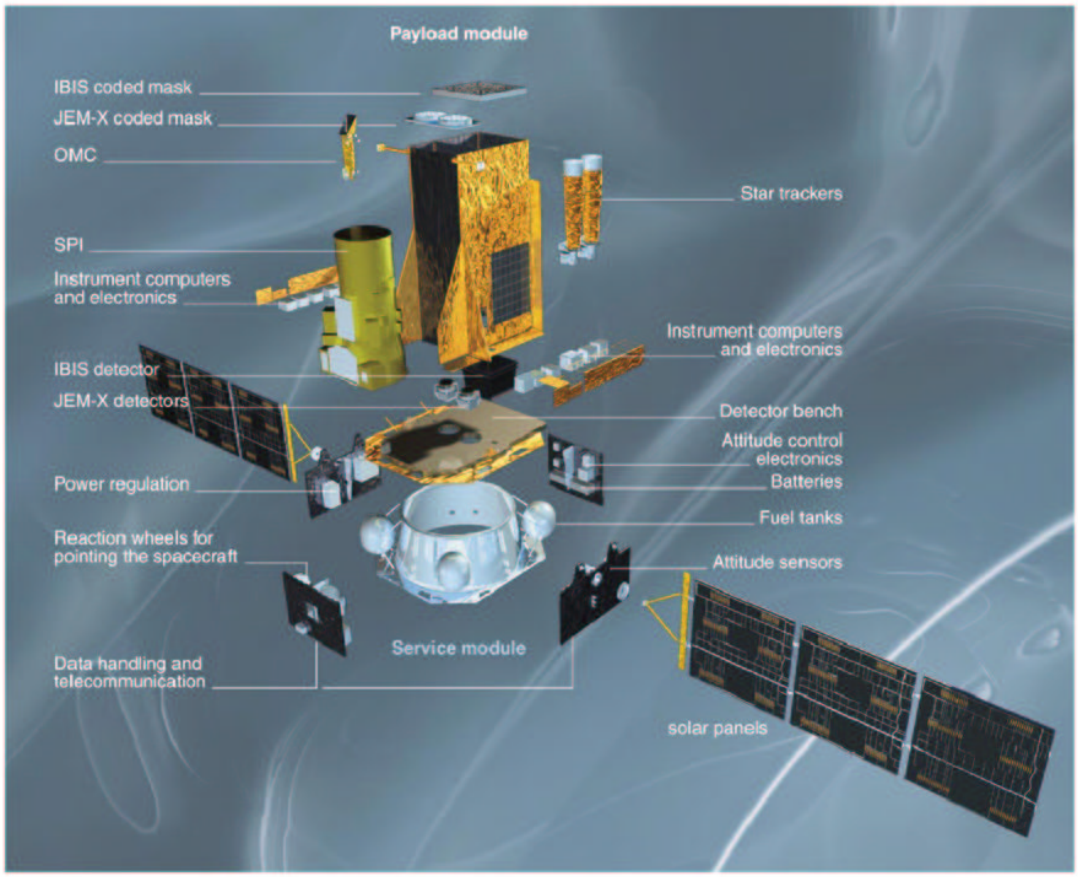

Figure 1: INTEGRAL Spacecraft

1.2 The Spectrometer (SPI)

The Spectrometer on INTEGRAL (SPI) is shown in Fig. 2. It employs an array of 19 germanium detectors cooled to an operating temperature of 85 K using a redundant pair of Stirling cycle mechanical refrigerators. The detector array operates over the energy range 20 – 8000 keV with an energy resolution that varies between $\sim$ 2 and 8 keV. This can be compared to the performance of scintillator-based instruments flown on the Compton Gamma-Ray Observatory having typical energy resolutions of 20 – 100 keV. The Ge detector array is surrounded by a massive (550 kg) active anti-coincidence shield made of BGO scintillator. The background in gamma-ray telescopes in space is produced by cosmic rays (primarily protons and alpha particles) that interact in the instrument and surrounding material. This background is usually very strong, requiring the use of extensive active shielding. The shield also acts as a collimator defining the total SPI field of view ($\sim 30^{\circ}$). A coded aperture array constructed from blocks of tungsten is used to produce coarse images (3° resolution).

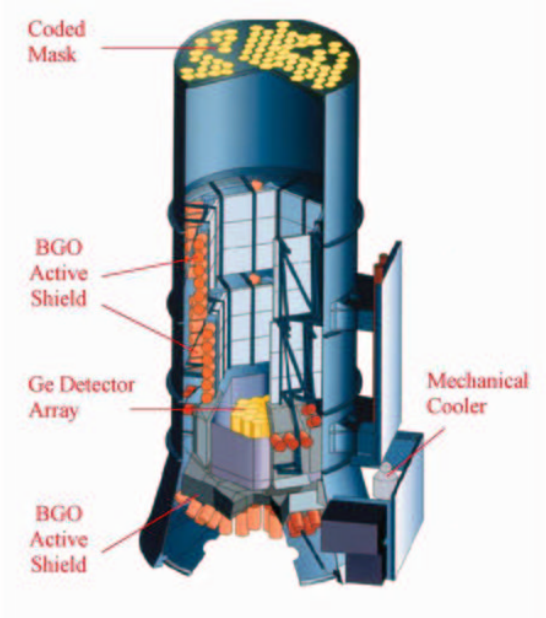

Figure 2: INTEGRAL Spectrometer (SPI)

1.3 The Imager (IBIS)

The INTEGRAL Imager (IBIS) is shown in Fig. 3. Similar in basic layout to the Spectrometer, it employs a two-layer detection plane consisting of large array ($\sim$16,000

detectors) of CdTe detectors and an array of CsI scintillator bars. The upper layer (ISGRI) is relatively thin and covers the energy range 15 – 1000 keV and the lower and thicker CsI layer (PICSIT) covers the range ∼150 – 10000 keV. Like the spectrometer, the Imager also has a coded-aperture, but one that is much more highly pixilated, achieving an angular resolution of 12 arcmin. A BGO shield surrounds the detector arrays and a passive tungsten collimator is used to restrict the field of view and prevent sources outside of the coded field-of-view from degrading the imaging performance. The Imager can observe sources as weak as $\sim$ 2 mcrab with a 10^5 sec exposure.

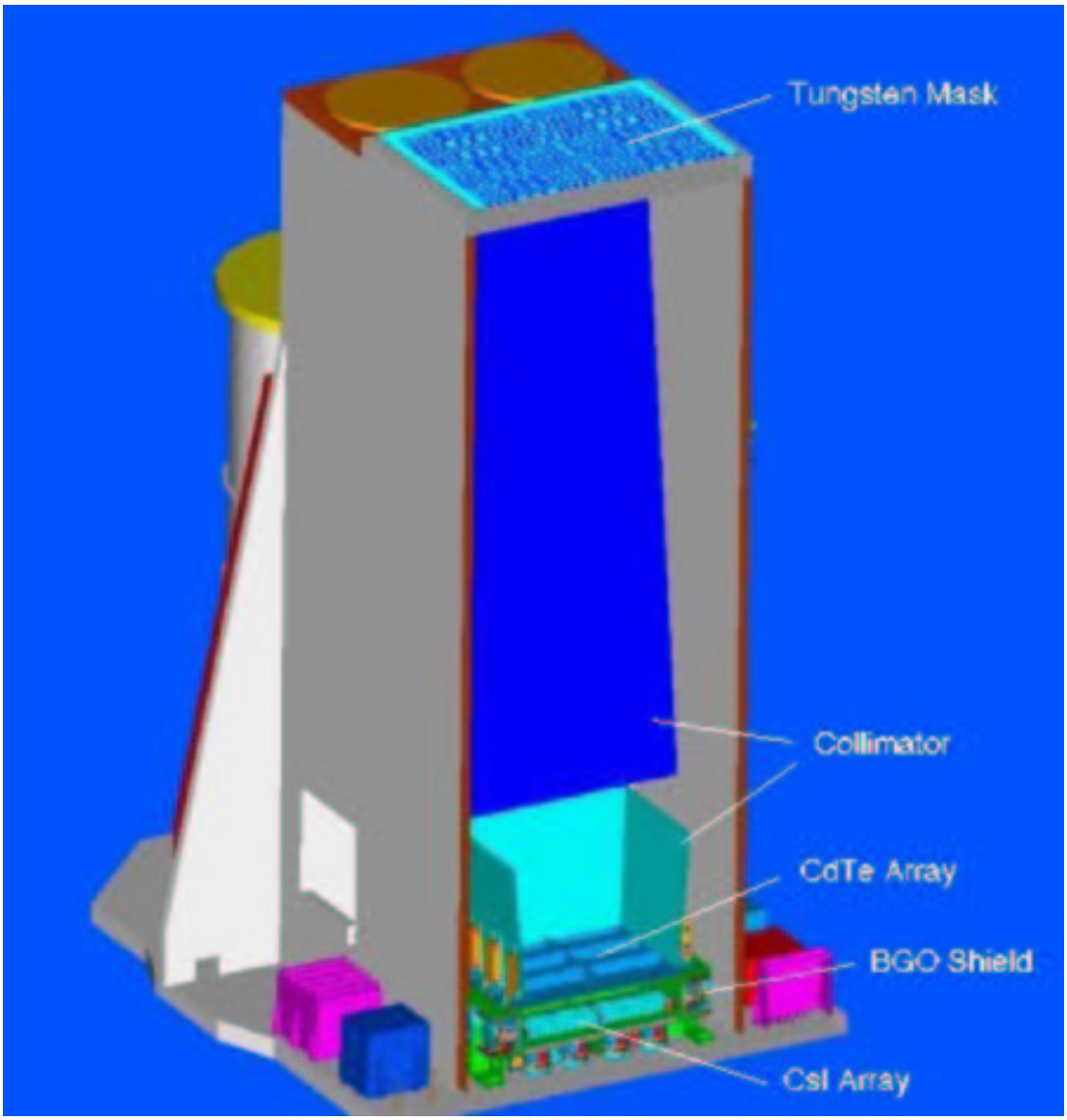

Figure 3: INTEGRAL Imager (IBIS)

1.4 INTEGRAL Observing Program

The INTEGRAL observing program is divided into two main parts, the Core Program and the Open Program. The Core Program is guaranteed time mainly for the instrument and data processing teams and comprises $\sim$ 1/3 of the observing time during the first three years of the mission and then drops to 1/4 for the remainder. It consists of three parts: 1) a deep observation of the central radian of our galaxy, 2) periodic (every 4 orbits) scans of the visible portion of the galactic plane with the primary goal of detecting new transient sources and 3) a few selected point source observations. The Open Program comprises the remainder of all of the observing time. The observations carried out under the Open Program are selected through an open competition held once each year. A breakdown of the observing program is shown in Fig. 4.

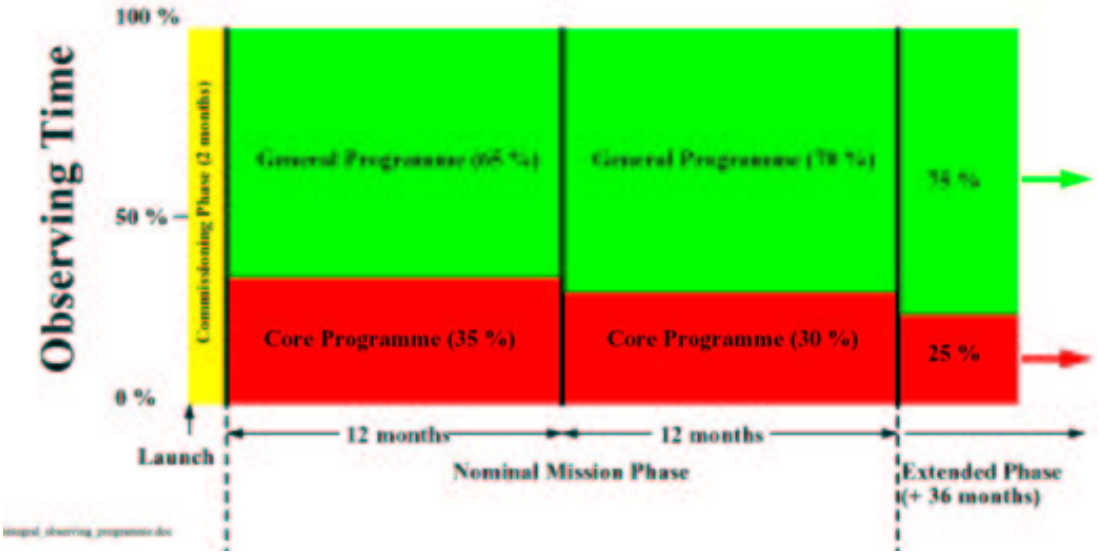

Figure 4: INTEGRAL Observing Program

2 THE CYGNUS REGION

2.1 Cygnus X-1

Cyg X-1, one of the brightest X-ray sources in the sky, was one of the two sources used for calibrating the INTEGRAL instruments. The Cygnus region was the first INTEGRAL target and was observed for more than 10^6 sec in Dec. 2002. Because of

the wide fields-of-view of the main instruments several other sources in addition to Cyg X-1 were detected. One of the first IBIS images of the Cygnus region in the 40-100 keV band is shown in Fig. 5. In addition to Cyg X-1, two other sources Cyg X-3 and J2103.5+4545 are clearly seen. Cyg X-1 is the first established binary black hole system.

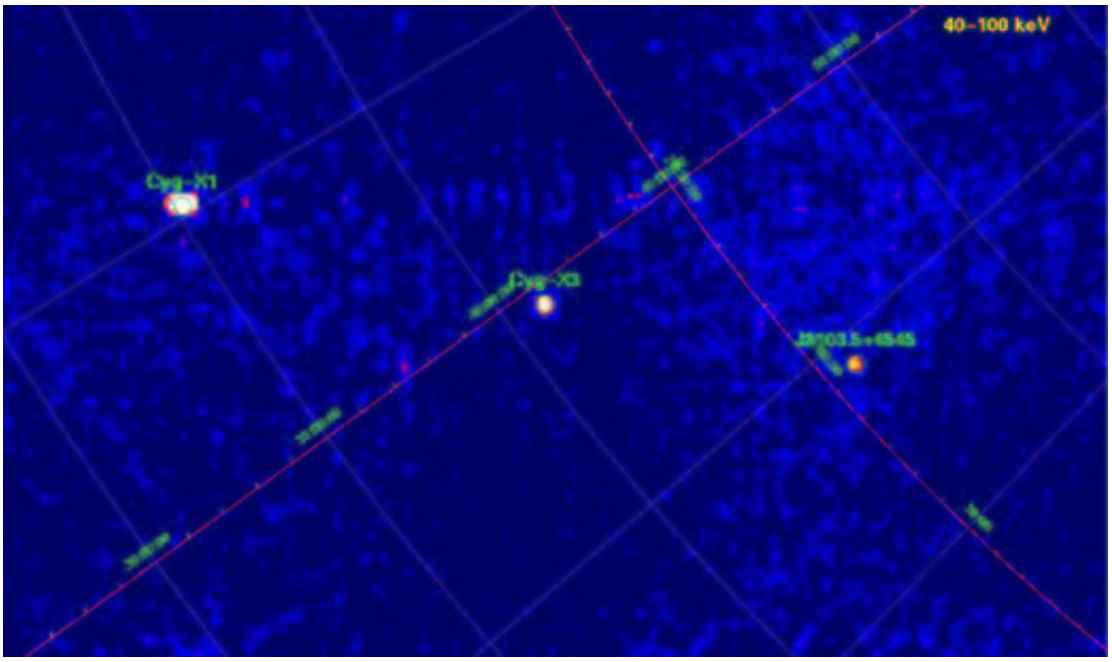

Figure 5: INTEGRAL/IBIS images of the Cygnus region.

The system consists of a black hole in orbit around a B0 supergiant star with a period of 5.6 days. The mass of the black hole has been determined from observations of the orbital variation to be ~ 7 M$_{sun}$.

Cyg X-1 is known to display complex temporal and spectral behavior. Variability on time scales from milliseconds to years has been observed, and at least 5 different spectral states have been seen. The temporal behavior of Cyg X-1 in the 20-40 keV band is shown in Fig. 6 for the first ~ 2 weeks of INTEGRAL observations.

Combined spectral observations of Cyg X-1 are shown in Fig. 7. Simultaneous observations of Cyg X-1 during the INTEGRAL Performance Verification period were carried out by RXTE (PCA + HEXTE). These are shown in Fig. 7 in two different time periods (revolutions 16 and 27) along with the integral data from JEM-X, IBIS and SPI. The normalizations of the spectra with respect to the PCA data have been allowed to float. With the exception of JEM-X they all lie within $\pm$20% of each other. The JEM-X normalization, however, was a factor of ~ 2 indicating lingering problems with

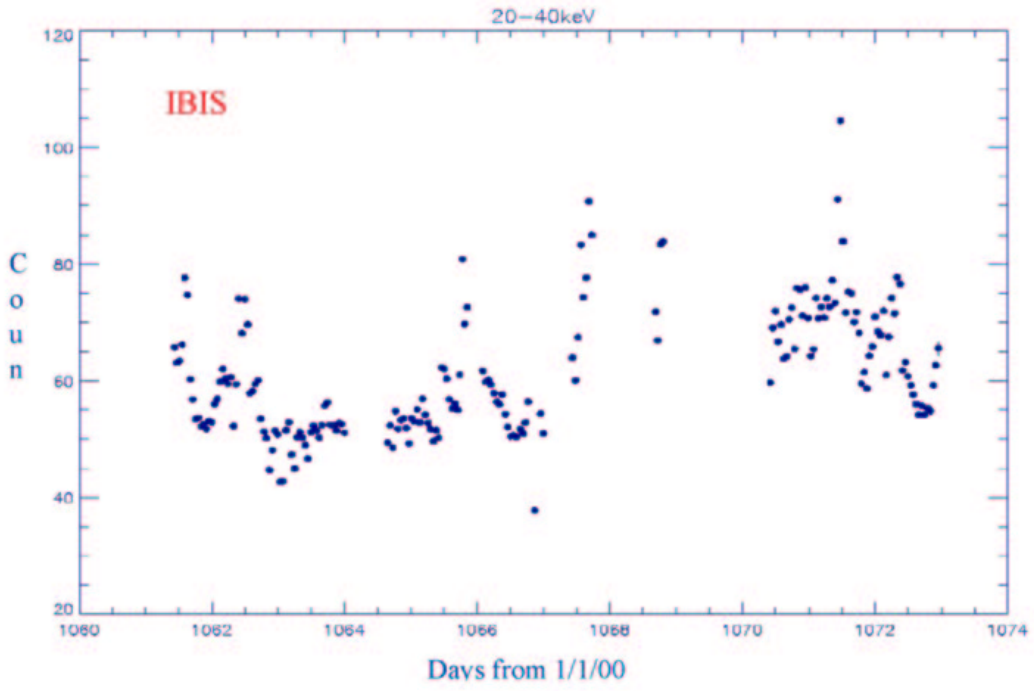

Figure 6: Time variation of Cyg X-1 as measured by INTEGRAL/IBIS during a 2-week period of the INTEGRAL Performance Verification period.

the calibration of that instrument. The spectra have been fit with a comptonization + reflection model shown as the solid lines in Fig. 7 producing the following best fit parameters: covering factor $\Omega \leq 0.3$, plasma temperature T_{plasma} = 80 keV and plasma optical depth τ_{plasma} = 1 – 1.5.

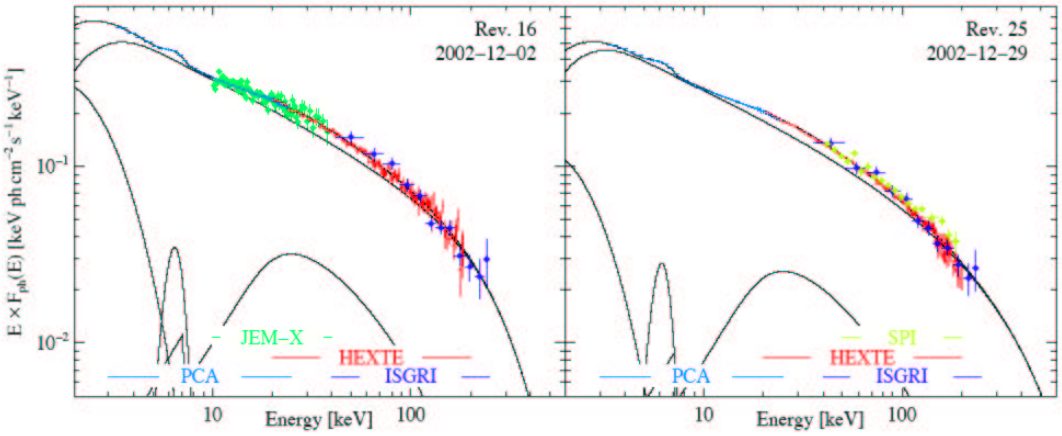

Figure 7: Cyg X-1 (Pottschmidt et al. 2003) spectra. Blue, RXTE/PCA; red, RXTE/HEXTE; green, INTEGRAL/JEM-X; purple, INTEGRAL/IBIS/ISGRI. Solid line is comptonization + reflection best-fit model.

2.2 Cygnus X-3

Cygnus X-3 is a peculiar micro-quasar (defined as a compact binary with a jet). Its X-ray flux displays a 4.8 hr modulation (see Fig. 8) that would lead to a conventional identification of this source as a low-mass X-ray binary (LMXB). Due to heavy obscuration no optical counterpart has been found. However, IR observations indicate the companion may be a high-mass Wolf-Rayet (WR) star. So the identification of this mysterious object remains uncertain. In Fig. 9 the residual phase lag of the Cyg X-3 light curve (days) is plotted as a function of time. Points from various earlier measurements are plotted along with the INTEGRAL. The INTEGRAL point is quite consistent with the earlier data.

2.3 EXO 2030+375

The transient source EXO 2030+375 was also detected during part of the INTEGRAL observation of the Cygnus region. EXO 2030+375 is a Be type X-ray transient (the most

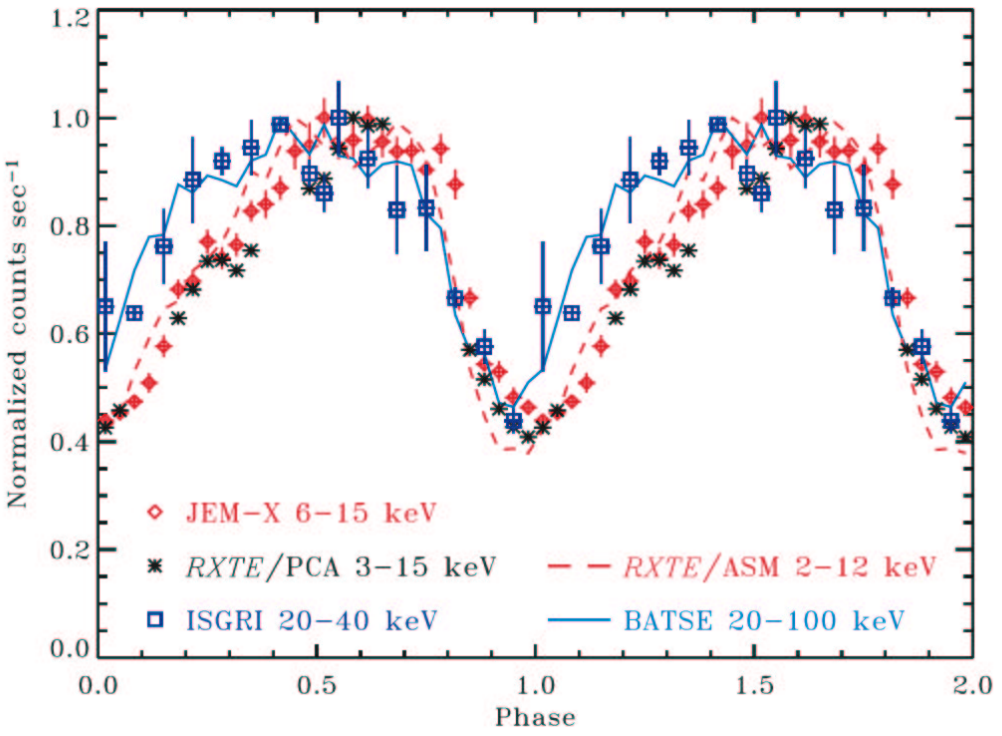

Figure 8: Cyg X-3 Light Curve (4.6 hr folding)

common type of X-ray pulsar) having a 42 sec spin period and a 42 day orbital period. Evidence for a cyclotron line at ∼36 keV has been reported by Rieg & Coe (1999). An IBIS/ISGRI light curve for the ∼ 2 week period when the source was visible is shown in Fig. 10. Also, shown is a light curve for the same period from the RXTE All-Sky Monitor (ASM). The strong correlation between the two data sets is apparent.

An IBIS/ISGRI spectrum for the source is shown in Fig. 11. The dip at ∼ 28 keV is an artifact of the spectral response. This is confirmed by the lower panel, which shows the ratio between the Crab and EXO 2030+375. No dip is seen in the ratio. The spectrum has been fit by a power-law with and exponential cut-off. The best-fit parameters are power-law spectral index = 1.5 ± 0.2, E_{cutoff}= 37 ± 4 keV, E_{fold}= 32 ± 4 keV. These are consistent with earlier observations (Reynolds et al. 1993).

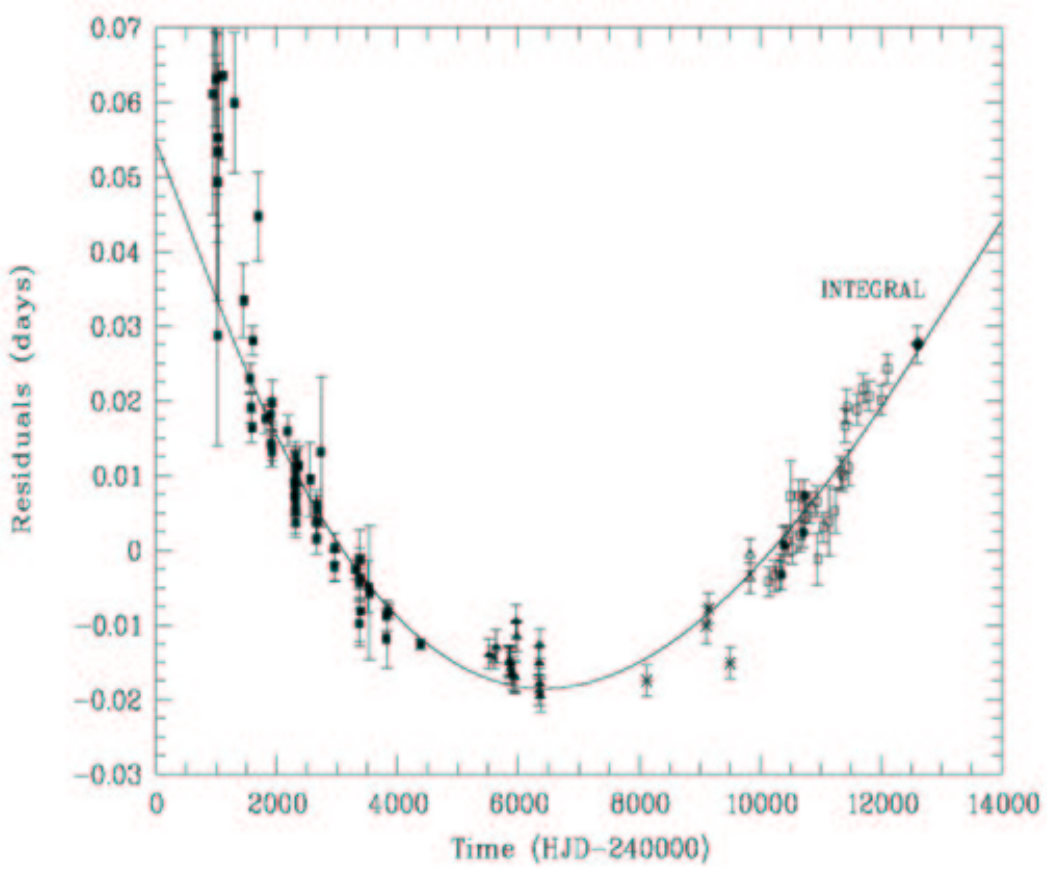

Figure 9: Cyg X-3. Time lag between measured minimum of light curve and linear ephemeris. Points other than INTEGRAL are taken from Singh et al. (2002)

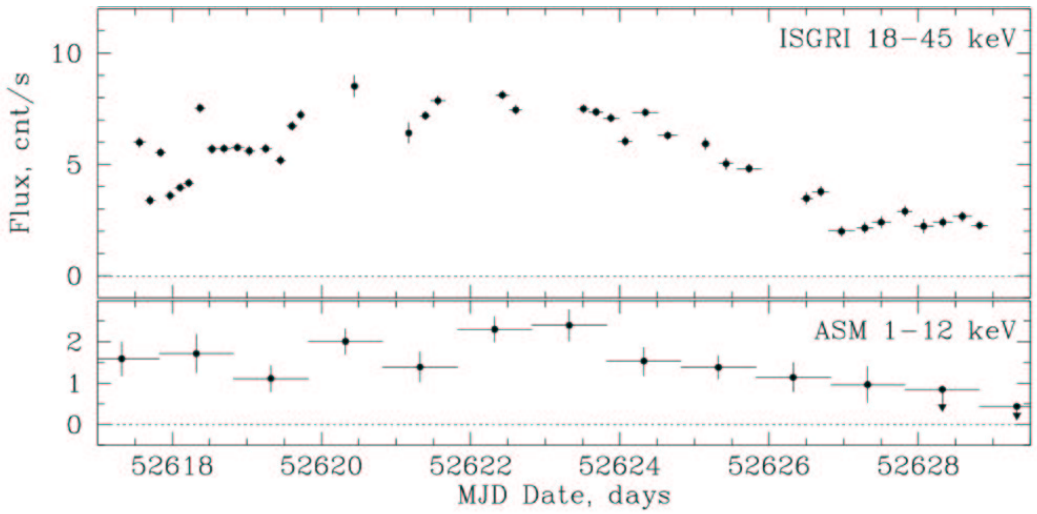

Figure 10: IBIS/ISGRI light curve of EXO 2030+375. Also shown is a light curve from the same period from the RXTE/ASM.

3 THE GALACTIC PLANE

3.1 Overview

Most of the INTEGRAL Core Program is devoted to observations in or near the Galactic Plane. There are two parts: 1) a deep exposure of the central radian and 2) regular scans of the visible portion of the plane. Using these data it been possible to construct maps of the sources in the Galactic Plane region. One example is shown in Fig. 12. The map is generated from IBIS/ISGRI data in the 15-40 keV band and is a snapshot of the central

portion of our galaxy taken in the period April 8-30, 2003. Roughly 40 discrete sources are visible. $\sim$ 10 of these are new sources discovered by INTEGRAL. The properties of the new INTEGRAL sources are summarized in Table 1. Some 12 sources are in the table including both those discovered in the Galactic Center Deep Exposure (GCDE) and the periodic Galactic Plane Scans (GPS). From the data in the Table 1. it can be seen that INTEGRAL can detect sources at least as weak as 5 mcrab.

3.2 A Possible New Class of Highly Absorbed Hard X-Ray Sources

Three of the new INTEGRAL sources in Table 1 are located near each other and have similar properties. IGR J16318-4848, IGR J16320-4751 and IGR J16358-4726 lie within a few degrees of each other in a region of enhanced concentration of massive stars

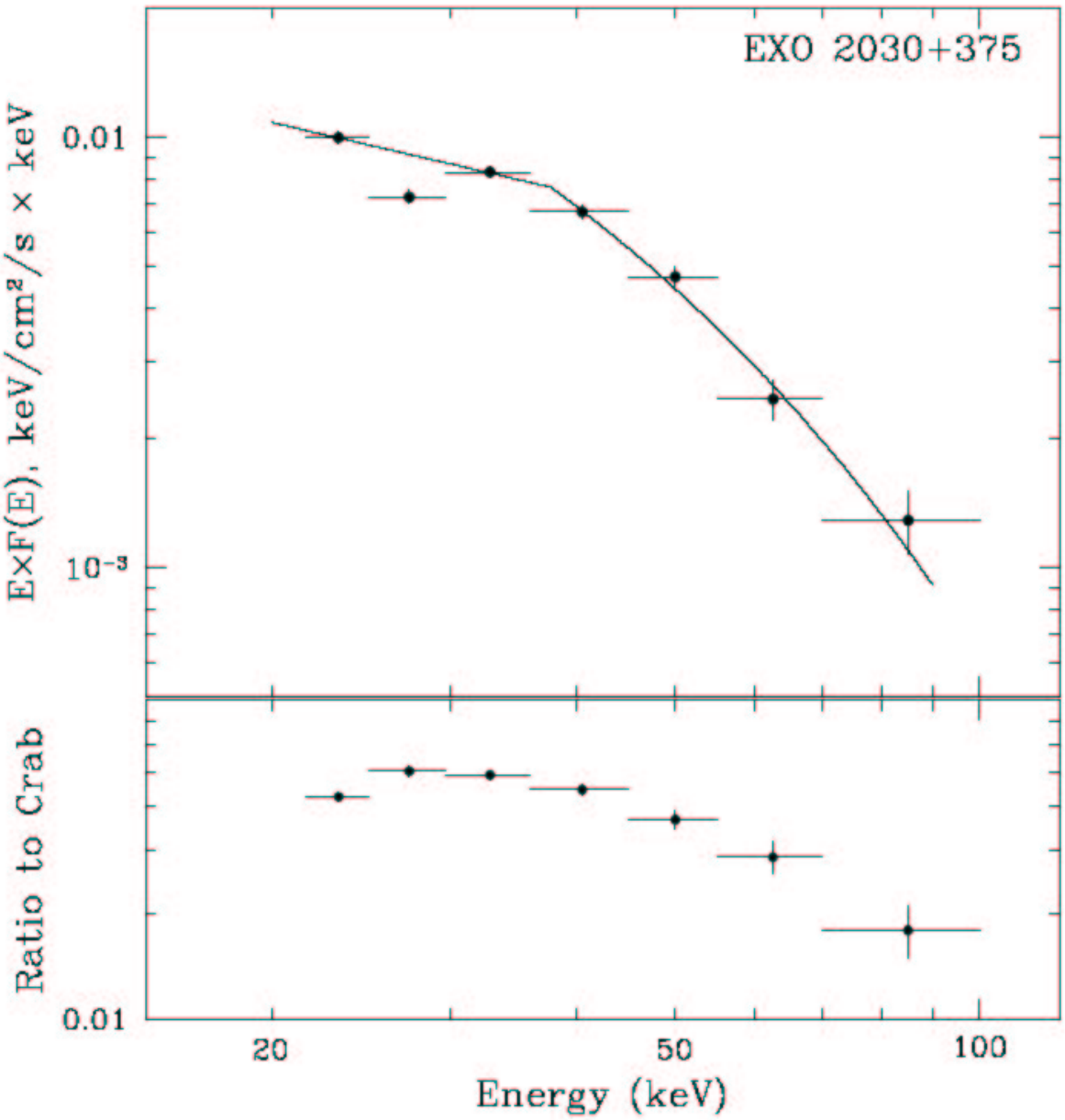

Figure 11: Upper panel: IBIS/ISGRI spectrum of EXO 2030+375. Lower panel: ratio of IBIS/ISGRI to Crab showing that the dip at ∼28 keV is an artifact.

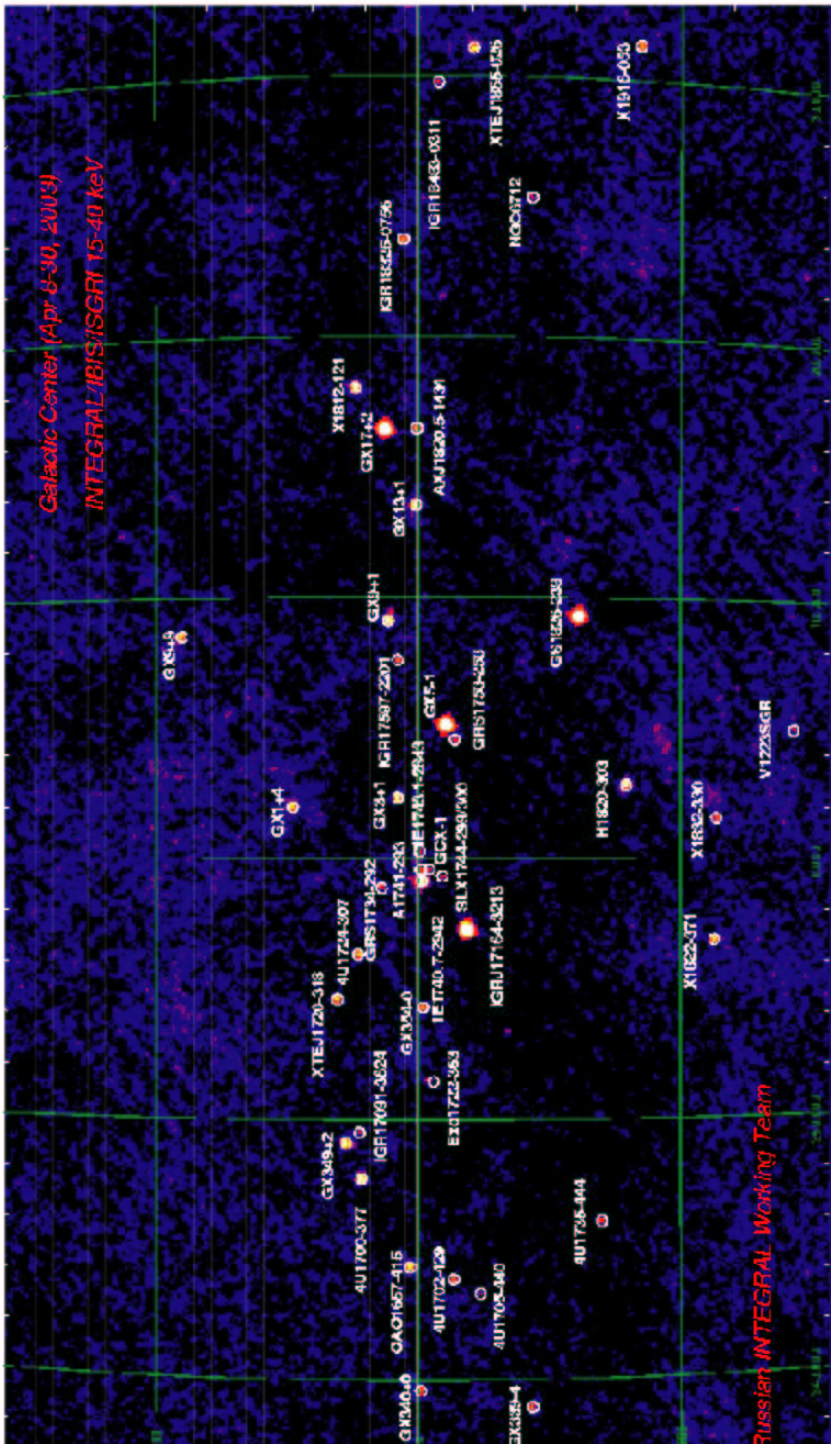

Figure 12: IBIS/ISGRI view of the central region of our galaxy.

Table 1: New INTEGRAL sources.

Source ID	Flux, 15-40 keV [mCrab]	Flux, 40-100 keV [mCrab]	Date	Reference
IGR J16318-4848	50-100	-	29-Jan-03	IAUC 8063
IGR J16320-4751	10-50	-	1-Feb-03	IAUC 8076
IGR J16358-4726	50	20	19-Mar-03	IAUC 8097
IGR J16479-4514	12 [18-25 keV]	8 [25-50 keV]	11-Aug-03	ATEL 176
IGR J17091-3624	-	20	19-Apr-03	ATEL 149
IGR J17464-3213	60	60	28-Mar-03	ATEL 132
IGR J17544-2619	160 [18-25 keV]	60 [25-50 keV]	17-Sep-03	ATEL 190
IGR J17597-2201	5 (S/N $\sim$ 10)	10 (S/N $>$ 14)	30-Apr-03	ATEL 155
IGR J18325-0756	10	5	28-Apr-03	ATEL 154
IGR J18483-0311	10 (S/N $\sim$ 21)	5 (S/N $\sim$ 11)	2-May-03	ATEL 157
IGR J18539+0727	20	20	21-Apr-03	ATEL 151
IGR J19140+098	50-100	-	6-Mar-03	IAUC 8088

in the Norma arm of our galaxy. The sources are all heavily absorbed. The best-fit values for an absorbed power-law fit to their spectra are given in Table 2 (Revnitsev 2003, Walter et al. 2003). All have exceptionally large values of the hydrogen absorption column N_H and similar spectral indices for the power-law component. XMM also observed the source IGR J16318-4848 and a combined spectrum is shown in Fig. 13. A model consisting of a power-law continuum and three Gaussian lines was fit to the data. The following Fe and Ni lines have been identified: Fe Kα (6.41 keV), Fe Kβ (7.07 keV) and Ni Kα (7.46 keV). A probable optical/IR counterpart has been found that could be either a low-mass red giant or a super-massive giant depending on the (unknown) reddening. Walter et al. (2003) suggest that the source is a binary system consisting of a massive star and a black hole in which a dense absorbing shell is created by a strong stellar wind.

4 GAMMA-RAY BURSTS

The INTEGRAL instruments are very sensitive to gamma-ray bursts ($\sim$ 3 x more sensitive than BATSE). However, the detection rates are not high ($\sim$ 1/mo.) due to the narrow fields-of-view of the telescopes. Nonetheless, INTEGRAL is a very useful trig-

Table 2: Properties of highly absorbed INTEGRAL sources.

Source	N_H (cm^{-2})	α [1]
IGR J16318-4848	3.1 x 10^{24}	1.0
IGR J16320-4751	2.1 x 10^{23}	1.2
IGR J16358-4726	4.0 x 10^{23}	1.1

[1] α = spectral index of power-law component

ger for providing burst alerts to the ground-based observer community in the interim period between the end of BeppoSax and the launch of Swift. Because of its high orbit INTEGRAL is sensitive to bursts $\sim$ 80% of the time. All INTEGRAL data is sent to the ground in real time making it possible to search for and detect gamma-ray bursts in near real time on the ground. The INTEGRAL Burst Alert System (IBAS) is a ground-based suite of software that continuously monitors the INTEGRAL data for gamma-ray bursts. If one is found then it automatically broadcasts an alert over the GCN (Gamma-Ray Coordinates Network) typically within 10 sec. of the detection. An example of a burst localized by INTEGRAL/IBAS is shown in Fig. 14 (Malaguti et al. 2003). Three nested error circles from INTEGRAL are shown from SPI, IBIS/ISGRI and IBIS/PICSIT, all consistent with common location. The smallest of these, that from IBIS/ISGRI has a diameter of 2 arcmin, small enough to permit virtually any ground-based telescope to make follow-up observations. This burst was also localized by multiple-spacecraft timing using the Interplanetary Network (IPN). The parallelogram-shaped error box is from the IPN and agrees quite well with the INTEGRAL position.

GRB030227 was the first burst detected by INTEGRAL for which it was possible to identify an optical counterpart. The optical counterpart was faint, $m_R \sim 23$ (Castro-Tirado et al. 2003). X-ray afterglow was detected by XMM (Mereghetti et al. 2003), the brightest detected by XMM for any gamma-ray burst, which may indicate that this was an "X-ray rich" gamma-ray burst. A composite optical, X-ray spectrum is shown in Fig. 15. The X-ray part lies well above an extrapolation of the optical part, which may be evidence for the presence of inverse Compton scattering.

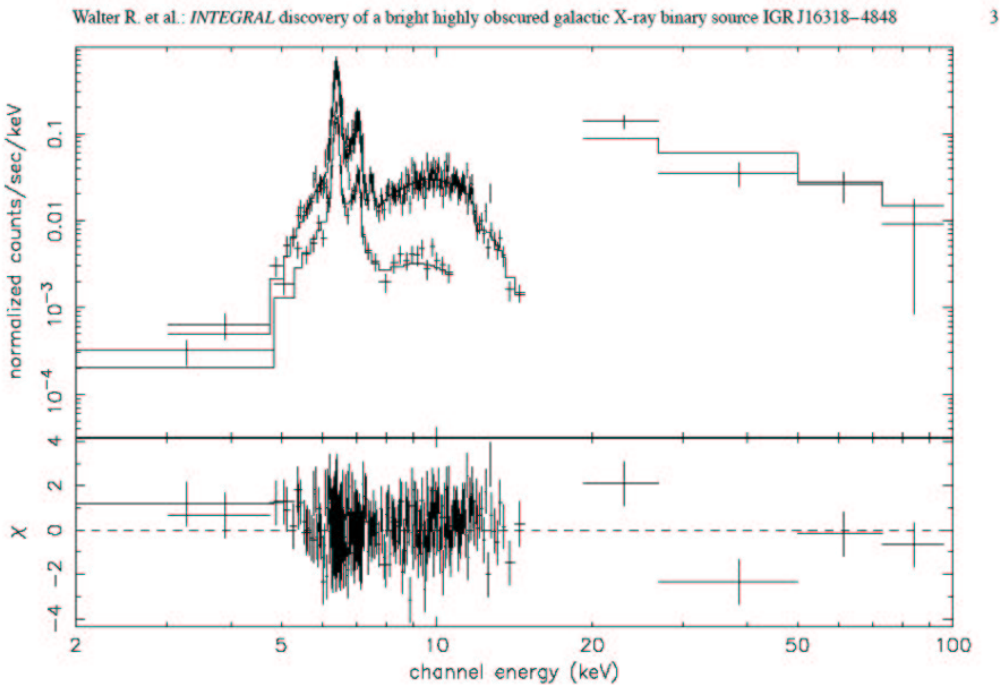

Figure 13: XMM (<20 keV) and INTEGRAL (>20 kev) spectra of IGR J16318-4848.

5 DIFFUSE GALACTIC PLANE LINE + CONTINUUM EMISSION

One of the primary objectives of the INTEGRAL mission is to map diffuse gamma-ray emission from the Galactic Plane. Of particular importance are the 511 keV electron-positron annihilation line and the 1809 keV line from radioactive ^{26}Al. The spectrometer SPI has been designed to map this emission on angular scales larger than a few degrees. The IBIS experiment can provide valuable information on point sources unresolved by SPI that might otherwise be included in the diffuse component. As of this writing the analysis of only the first season (spring '03) of Galactic Center observing is complete. This represents only a very small fraction of the data on the Galactic Center and Plane that will eventually be accumulated.

5.1 ^{26}Al Line Emission

The1809 keV from^{26}Al decay with its $\sim$ million year half-life is a valuable tracer of recent nucleosynthesis in our galaxy. The spatial distribution of the emission has been

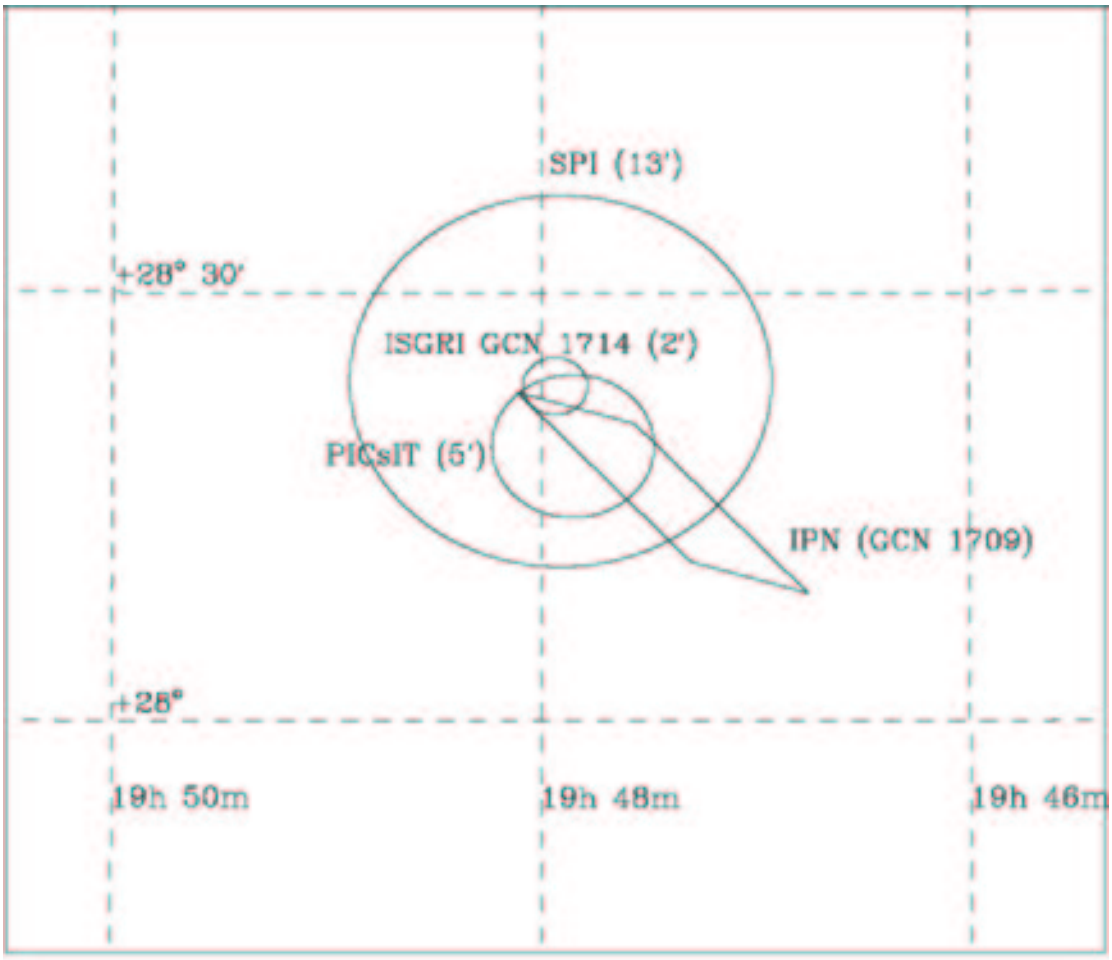

Figure 14: Error boxes for GRB021125. Ellipses are from smallest to biggest IBIS/ISGRI, IBIS/PICSIT and SPI. The parallelogram is from the IPN.

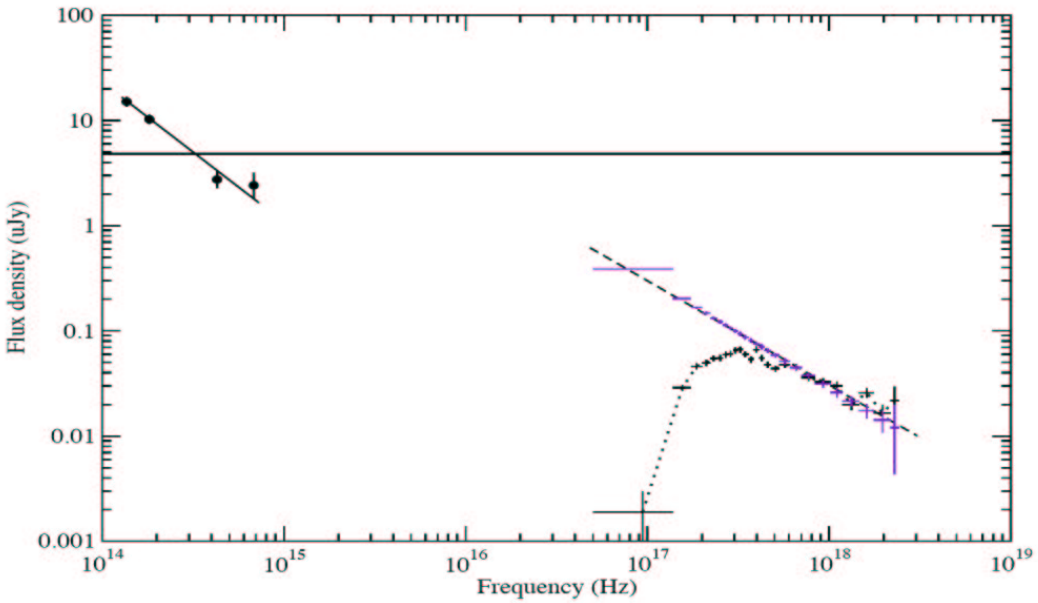

Figure 15: Composite optical + X-ray spectrum of GRB030227 afterglow (Castro-Tirado et al. 2003). Also shown (purple) is a "de-adsorbed" X-ray spectrum, which is the power-law component of a best-fit absorbed power-law model.

measured by the COMPTEL experiment on CGRO (Diehl, Knodlseder, Plushke) and is primarily concentrated within $\pm$ 5° of the Galactic Plane (see Fig. 16). Significant enhancements in the emission are evident in the Cygnus, Carina and Vela regions. The ^{26}Al distribution tracks that of microwave emission, which is primarily due to free-free electron interactions. Free electrons are produced by UV radiation from massive stars and thus trace massive star formation in our galaxy. ^{26}Al is produced in the cores of these stars, transported by convection to the surface and then injected into the interstellar medium by strong stellar winds.

The INTEGRAL/SPI 1809 keV line profile is shown in Fig. 17 (Diehl et al. 2003). It was derived by fitting a profile from galactic free-free emission (DIRBE 240 μm) to the data in each 1 keV energy bin. The preliminary integrated flux value is 3-5 $\times 10^{-4}$ cm^{-2} s^{-1}, the range being determined by the particular assumed model. This is consistent with most earlier measurements. The preliminary limit for the line width is $<$ 3 keV. A balloon-borne germanium detector (GRIS) measurement of the ^{26}Alline width of $\sim$6 keV (Naya et al. 1996) suggested velocities of the emitting matter of the order of 500 km s^{-1}. However, a more recent determination of this width by the RHESSI satellite (Smith et al. 2003) did not find evidence for any line broadening. The spatial regions covered

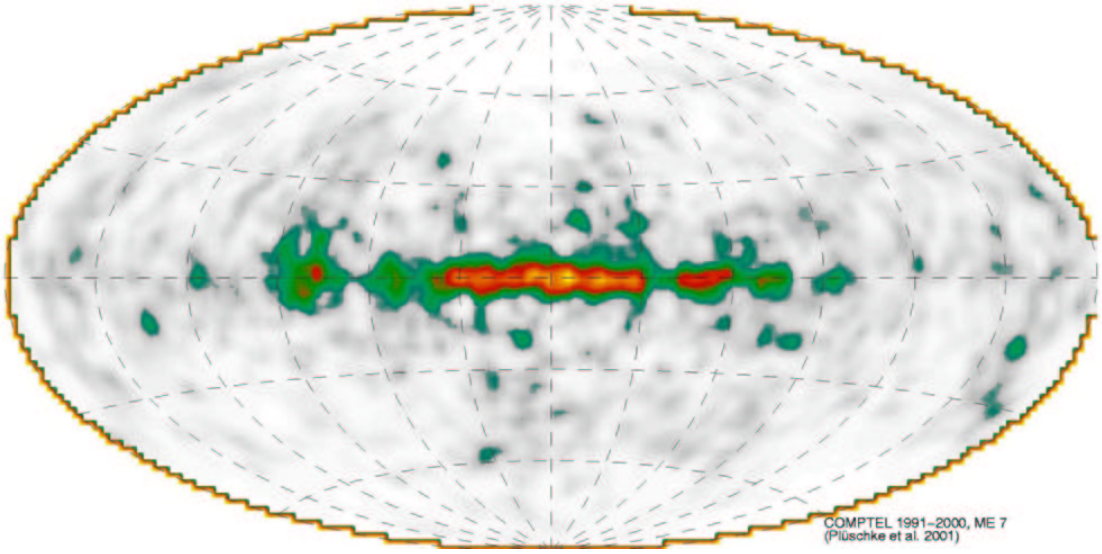

Figure 16: Diffuse ^{26}Al Map of our Galaxy (Pluschke et al. 2001).

by GRIS, RHESSI and SPI are not the same, which could account for the differences in line width. With its high sensitivity, fine energy resolution, and imaging capability INTEGRAL/SPI will surely settle the question of the ^{26}Alline width.

5.2 Electron-Positron Annihilation Radiation

The center of our galaxy has been known for more than twenty years to be a strong source of electron-positron annihilation radiation (see e.g. Leventhal et al. 1980, Purcell et al. 1997, Teegarden et al. 1997). The signature is a narrow line at the electron rest energy (511 keV) due to two-photon decay accompanied by a broad positronium continuum below 511 keV from three-photon decay. Early balloon measurements suggested that the radiation was time variable (Leventhal et al. 1980, Paciesas et al. 1982), however, this was not confirmed by later satellite results (Purcell, Harris). The line width of $\sim$ 2 keV is just barely resolved by the germanium spectrometers. The OSSE experiment on CGRO has produced maps of the e+ - e- emission vicinity of the Galactic Center (Purcell et al. 1997, Milne et al. 2001). One of these is shown in Fig. 18 (Purcell et al. 1997). The emission can be described as consisting of three components:

1) a central symmetric bulge of width $\sim 10^{\circ}$, 2) a plane component of width $\sim 30^{\circ}$ and height 5°–10°, and 3) a positive latitude enhancement (the so-called “Galactic Fountain”) centered at l $\sim$ –2°, b $\sim 7^{\circ}$. The fountain was not present in all of the different OSSE maps (Milne et al. 2001), and its existence remains controversial. The

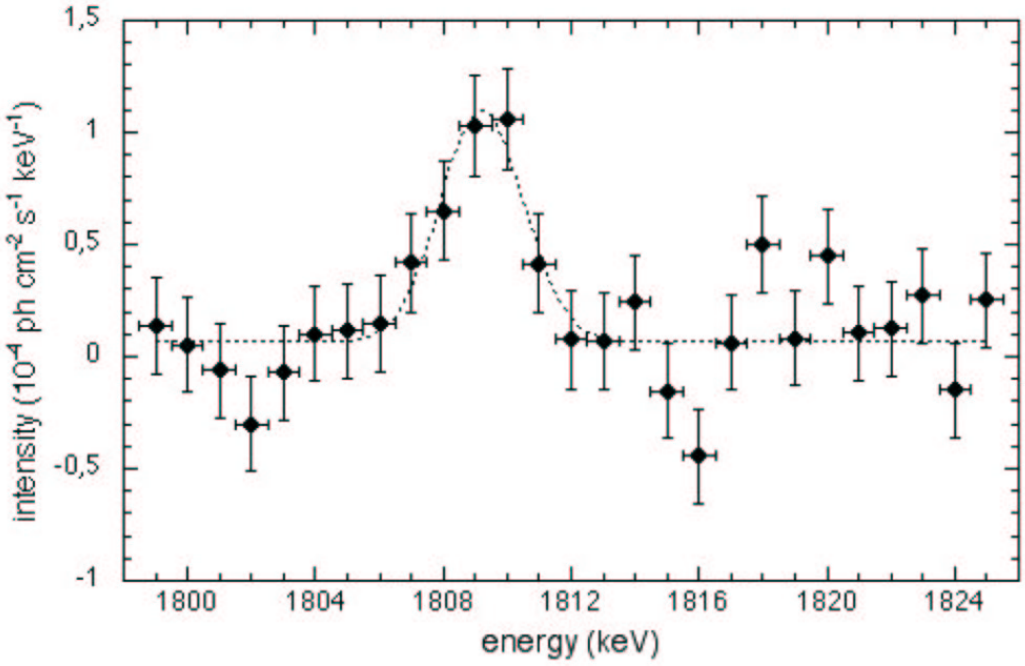

Figure 17: ^{26}Al (1809 keV) line profile. Values are obtained by fit to spatial model based on DIRBE 240 μm map.

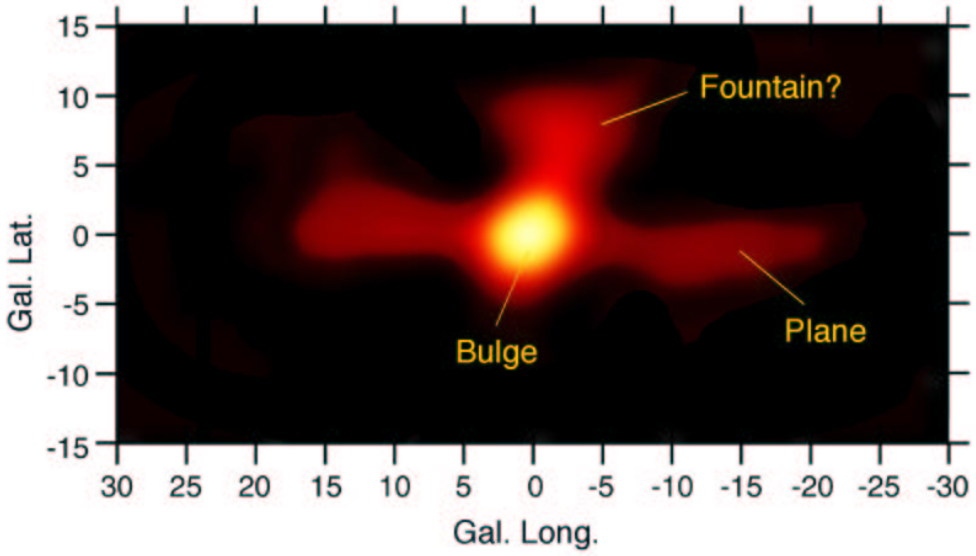

Figure 18: OSEE map of e+ - e- emission from the vicinity of the Galactic Center (Purcell et al.)

first INTEGRAL/SPI map of the Galactic Center region is shown in Fig. 19 (Knodlseder et al. 2003). The map was created using a Richardson-Lucy deconvolution smoothed with a $6^\circ \times 6^\circ$ boxcar kernel. Because of data sharing agreement with the Russians it is only possible to show the 4^{th} quadrant ($-90^\circ < l < 0^\circ$) in this paper. The map is consistent with a symmetric bulge component with a diameter of $\sim 10^\circ$ which in turn is consistent in extent and flux with the OSSE bulge component. Neither the disk nor the fountain component is visible in Fig. 19, however with the small amount of data available in this map it is probably not possible to resolve these components if they are present at the levels reported by OSSE.

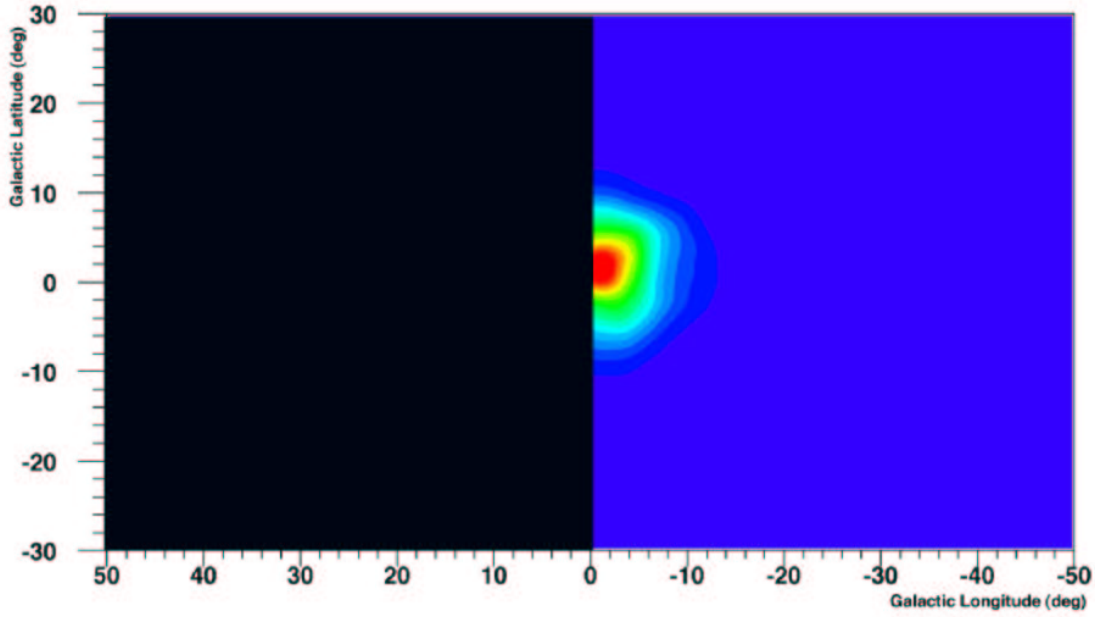

Figure 19: INTEGRAL/SPI map of the 511 keV emission in the 4th quadrant of the Galaxy.

To determine the profile of the 511 keV line a spatial model consisting of a symmetric Gaussian centered at l = 0°, b = 0° with FWHM of 10° was fit to the data separately in each 1 keV energy bin. The results of that fit are shown in Fig. 20. The line parameters are given in Table 3 and compared with previous measurements. The SPI flux and centroid are quite consistent with previous observations with no evidence for any red or blue shift of the line. The SPI line width is at the high end of the range covered by the prior observations, but in all cases the differences are less than 2σ.

Table 3: Galactic Center 511 keV Line Results

Instrument	Flux [10-3 cm-2 s-1]	Centroid [keV]	Width (FWHM) [keV]	Reference
HEAO-3	1.13 ± 0.13	510.92 ± 0.23	1.6 +0.9/-1.6	Mahoney et al. 1994
GRIS	0.88 ± 0.07		2.5 ± 0.4	Leventhal et al. 1993
HEXAGONE	1.00 ± 0.24	511.33 ± 0.411	2.90 ± 1.1	Smith et al. 1993
TGRS	1.07 ± 0.05	510.98 ± 0.10	1.81 ± 0.54	Harris et al. 1998
SPI	0.99 +0.47/-0.21	511.06 ± 0.19	2.95 +0.45/-0.51	Jean et al. 2003

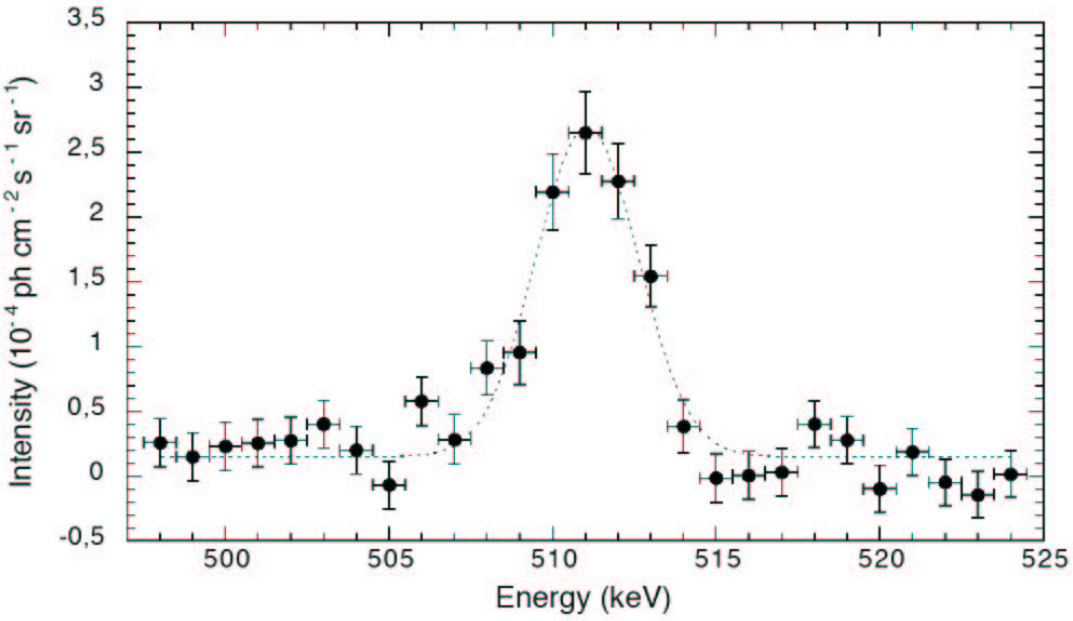

Figure 20: SPI spectrum from the Galactic Center of the 511 keV e^+ - e^- annihilation line.

5.3 Diffuse Galactic Plane Continuum

The Galactic Plane is a strong source (total luminosity $\sim 10^{38}$ erg cm^{-2}) of "diffuse" hard X-ray and gamma-ray continuum emission. Diffuse here is in quotes because it is not yet clear whether part or all of the continuum is due to an aggregate of unresolved point sources. The total luminosity of $\sim 10^{38}$ erg cm^{-2} is quite strong. Using a procedure similar to the model fitting for the 1809 keV line Strong et al. (2003) have derived a Galactic Plane spectrum shown in Fig. 21. The spectrum is well fit by a power-law (red) with an exponential cut-off combined with a positronium continuum (green). The positronium continuum is required at a high level of significance. The positronium fraction is defined as the fraction of those annihilations that proceed through the formation of positronium. This fraction is a telltale indicator of the condition of the medium in which the annihilation took place. Comparison of the data in Fig. 21 with the INTEGRAL/SPI 511 keV narrow line flux (see Fig. 20) yields a positronium fraction $f_p > 90\%$, which is consistent with most prior results.

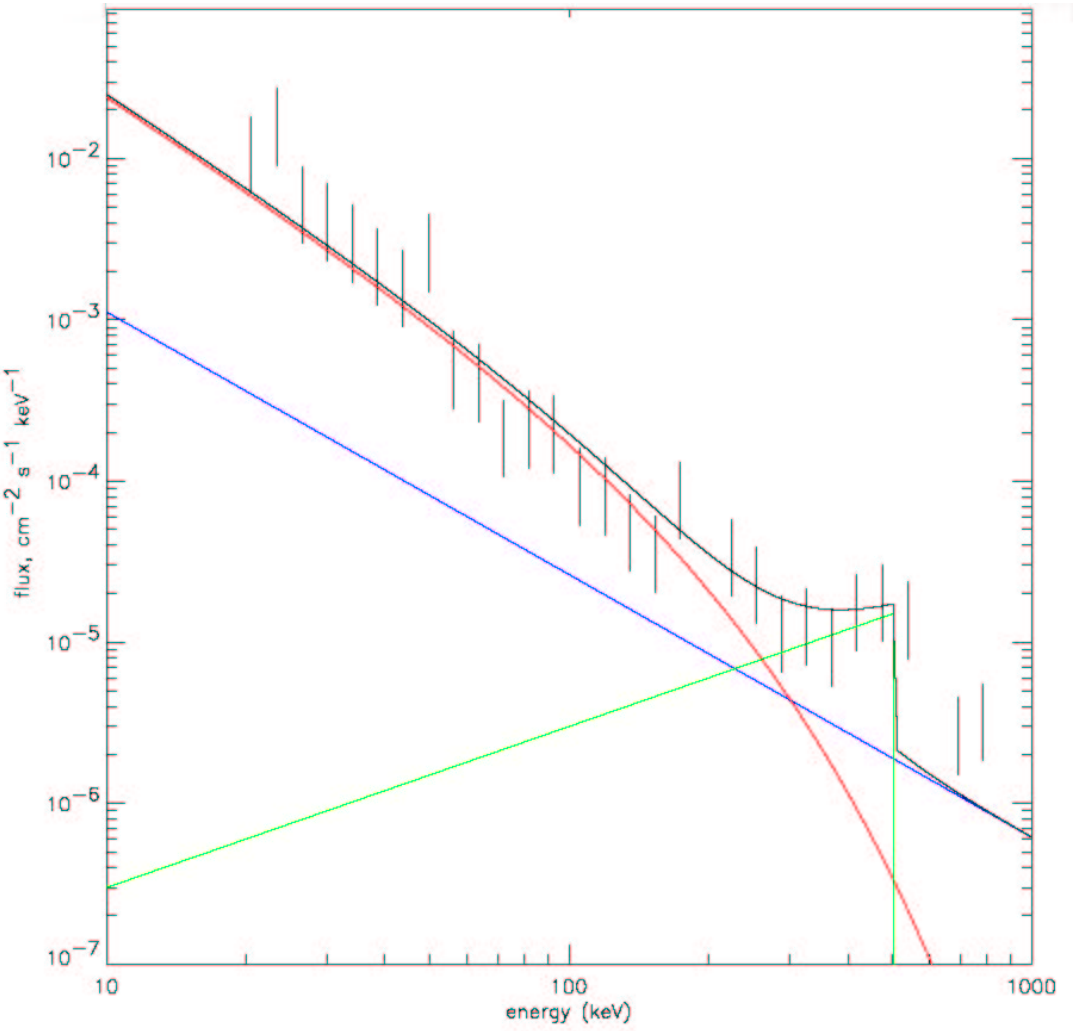

Figure 21: SPI Galactic Plane continuum spectrum. Best fit spectrum: power-law with exponential cut-off (red) + power-law (blue) + positronium continuum (green).

References

[1] Castro-Tirade et al. 2003, A&A, in press.

[2] Diehl, R. et al. 1995, A&A, **298,** 445.

[3] Diehl, R. et al. 2003, A&A, in press.

[4] Goldoni, P. et al. 2003, A&A, in press.

[5] Jean, P. et al. 2003, A&A, in press.

[6] Knodlseder, J. et al. 1999, A&A, **344**, 68.

[7] Knodlseder, J. et al. 2003, A&A, in press.

[8] Harris et al. 1998, ApJ, **501,** L55.

[9] Leventhal, M. et al. 1980, ApJ, **240**, 338.

[10] Mahoney et al. 1994, ApJ Supp, **92**, 387.

[11] Malaguti, G. et al., 2003, A&A, in press.

[12] Mereghetti S. et al. 2003, A&A, in press.

[13] Milne, P. et al. 2001, AIP Conference Proceedings, **587**, 11.

[14] Naya, J. et al. 1996, Nature, **384**, 44.

[15] Paciesas, W. et al. 1982, ApJ, **260**, L7.

[16] Pluschke, S. et al. 2001, In: Exploring the Gamma-Ray Universe (4th INTEGRAL Workshop), (Eds.)A. Gimenez, V. Reglero and C. Winkler. ESA SP-459, Noordwijk, The Netherlands, 55-58.

[17] Purcell, W. et al. 1997, ApJ, **491**, 725.

[18] Reig, P. & Coe, M. J. 1999, MNRAS, **302**, 700.

[19] Revnitsev, M. 2003, Astronomy Letters, in press.

[20] Reynolds, A. P., Parmar, A. N. & White, N. E. 1993, ApJ, **414**, 302.

[21] Singh, N. S. et al. 2002, A&A, **392**, 161.

[22] Smith, D. et al. 2003, ApJ, **589**, L55.

[23] Strong, A. et al. 2003, A&A, in press.

[24] Teegarden et al. 1997, ApJ, **463**, L75.

[25] Walter, R. et al. 2003, A&A, in press.